The Effect of Platinum Based Bimetallic Electrocatalysts on Oxygen Reduction Reaction of Proton Exchange Membrane Fuel Cells

Kyuhwan Hyun[1], Jin Hee Lee[2], Chang Won Yoon[2], and Yongchai Kwon[1,]*

[1]Graduate school of Energy and Environment, Seoul National University of Science and Technology, 232 Gongneung-ro, Nowon-gu, Seoul, 139-743, Republic of Korea
[2]Fuel Cell Center, Korea Institute of Science and Technology, Hwarangno 14-gil 5, Seongbuk-gu, Seoul, 139-791, Republic of Korea
[*]E-mail: kwony@seoultech.ac.kr

Carbon supported PtM (M = Ni, Co, Cu and Y) alloy catalysts (PtM/Cs) are synthesized by reduction of metal precursors using sodium borohydride. With the PtM/Cs adopted as cathodic catalyst for proton exchange membrane fuel cells (PEMFCs), their oxygen reduction reaction (ORR) activity, catalytic stability and electrical performance are evaluated and compared with those of commercial Pt/C. Their crystal structure and elementary composition are measured by XRD, EDX and TEM. The measurements show that PtM/Cs have similar particle size to Pt/C and moderate PtM alloying degree. For evaluating ORR activity, catalytic stability and electrical performance, cyclic voltammetry, rotating disk electrode and PEMFC single cell tests are used. In terms of catalytic stability, PtM/Cs are more stable than Pt/C. It is probably due to higher adsorption energy for oxygen-M bond and lower M-M bond energy. In ORR activity and electrical performance tests, PtNi/C shows better limiting current density, kinetic current density, half wave potential, reduction peak potential and maximum power density than Pt/C despite less amount of Pt in PtNi/C than that in Pt/C. However, when the measurements are analyzed as per gram Pt, all the PtM/C catalysts indicate better results than Pt/C, turning out that Pt particles in PtM/C are more effectively utilized than those in Pt/C.

1. INTRODUCTION

Importance of the proton exchange membrane fuel cell (PEMFC) as a primary power source is getting increase owing to its superior features such as high energy efficiency, low pollution, light

weight and room temperature operation [1,2]. However, despite such kinds of advantages, more advances of the PEMFC have been retarded than expected mainly due to a sluggish oxygen reduction reaction (ORR) that is a rate determining step determining an overall efficiency of the PEMFC. Namely, efficiency loss by the slow ORR kinetics occurring in cathode electrode during operating of the PEMFC corresponds to 80% of the entire loss. It is related to performance degradation by excessive cathodic overpotential (0.3-0.4 V) that takes place on the surface of platinum (Pt) catalyst [1-5].

The Pt has been long considered as a typical cathodic catalyst for ORR of PEMFC and has still been widely used as the first option of the cathodic catalyst compared to other candidates. However, besides high overpotential, the Pt catalyst has other drawbacks to address like expensive cost, decrease in catalytic activity by CO poisoning and short catalytic stability [6-8].

(i) To curtail the overpotential, (ii) to minimize the consumption of expensive Pt, (iii) to increase the ORR activity and (iv) to improve the catalytic stability, many efforts have been made to date. Searching for a proper alternative being able to replace the Pt catalyst was one of the efforts is to [6-11].

As the most viable approach in that direction, alloying Pt with other metals (Ni, Co, Cu, Fe, Y, Pd, Ti, Cr etc.) (PtM) has been suggested [6-13]. From the previous research, it was reported that some PtM catalysts facilitated an increment in ORR activity as well as a reduction in overpotential. Such enhancements in the ORR activity were mainly explained as follows: (i) change in the orbital structure of PtM like electron occupancy between d_{z2} and d_{xy}-d_{yz} orbitals, (ii) change in Pt-Pt interatomic distance by employment of the adatom, (iii) adsorption and desorption behavior of oxygen-containing species like hydroxyl molecules bound onto the surface of PtM [9,14,15]. In a bid to synthesize the PtM alloying, several methods such as impregnation, polyol, solverthermal, sputtering and nanocapsule have been tried [1,6,13,16,17]. However, determining proper PtM structure and PtM synthetic route has not been completed yet and it is therefore instrumental to elucidate the excellent alloy and synthetic method.

As the related research, Toda *et al.* prepared for three different PtMs (PtCo, PtFe and PtNi) catalysts by a radio frequency (rf) magnetron sputtering and obtained better ORR activities in PtM catalysts than Pt catalyst [1]. The authors explained the Pt adatoms promoted an increase in d band vacancies, resulting in enhanced 2π electron donation from O_2 to the surface of PtM. By both the donated electrons and back donation of the electrons, O_2 reacted with four electrons and protons to produce fast and desirable two H_2O molecules. Yano *et al.* synthesized five different PtM catalysts (PtCo, PtCr, PtNi, PtV and PtFe) on the carbon supporting material by nanocapsule method [13] and they proved that the newly synthesized catalysts led to smaller particle size than a commercial Pt/C and uniform alloy composition, and the well-arranged alloy catalysts produced excellent ORR activities. Xiong *et al.* made four PtMs (PtCo, PtCu, PtNi and PtFe) by sodium formate (HCOONa) reduction and the PtMs showed better activity for ORR than Pt. In particular, they discovered the effect of post heat treatment on ORR activity of PtMs [11]. Wang *et al.* prepared three Pt_3Ms (Pt_3Co, Pt_3Ni and Pt_3Fe) by organic solvothermal method [18]. According to the authors, such synthesized Pt_3Ms demonstrated monodisperse and homogeneous alloy compounds and led to improvements in the parameters affecting ORR activity (i.e., particle size, alloy composition, and catalyst pretreatment).

Of the possible Pt bimetals, 3d transition metals like Ni, Co, Cu (PtNi, PtCo and PtCu) and Y (PtY), which is being shed new light on, are intriguing combinations as the cathodic catalyst for ORR due to their excellent electrical and structural superiorities. Due to the reasons, the PtMs have been individually served as catalyst candidates for ORR of PEMFC [1,2,17]. However, a simultaneous study of the four PtMs (PtNi, PtCo, PtCu and PtY) as cathodic catalysts for the ORR of PEMFC has not been reported, although comparison amid the four PtMs synthesized at the similar condition might be meaningful for determining a proper catalyst.

In the present study, we synthesized the four different PtMs on the carbon supporter (Vulcan XC-72R) and utilized them as cathodic catalysts for the ORR. ORR activity, catalytic stability and electrical performance of the carbon supported PtMs (PtM/Cs) were measured by using both half-cell and single-cell experiments and their evaluations were compared with those of the commercially available Pt/C (40 wt% Pt on Vulcan XC-72R).

To characterize the electrochemical performances of the PtM/C and Pt/C catalysts, the following five ways were carried out. First, X-ray diffraction (XRD) and energy density X-ray spectroscopy (EDX) are used to detect crystal structure and to measure elementary composition and alloying degree of the PtM/C. Second, TEM images were obtained to observe the extent of dispersion of metal particles in the PtM/C. Third, cyclic voltammetry (CV) curves were measured to estimate electrochemically active surface area (EAS), ORR activity in the presence of O_2 gas and catalytic stability in the presence of N_2 gas. Fourth, linear sweep voltammetry (LSV) curves using rotational disk electrode (RDE) were measured to attain half wave potential, limiting current density and transferred electron number. Fifth, performances of the PEMFC single cells that adopted PtM/C and Pt/C as cathodic catalysts were measured to evaluate the effect of PtM/Cs on ORR and PEMFC performance.

2. EXPERIMENTAL

2.1 Synthesis of catalysts

The carbon supported PtM (M = Ni, Co, Cu and Y) alloy catalysts (PtM/C) were prepared by a modified impregnation method where metal precursors are reduced by sodium borohydride ($NaBH_4$) and anhydrous ethanol. In an initial step, 0.15 g of carbon black powders (Vulcan XC-72R) were mixed with 180 mL ethyl alcohol and the solution was held for 30 min under sonication. After the sonication, the proper amounts of platinum (IV) chloride and M metal precursors (nickel (II) chloride hexahydrate for Ni, cobalt (II) chloride hexahydrate for Co, copper (II) nitrate hemi (pentahydrate) for Cu and YCl_3 for Y) were dissolved with 1.423 g of sodium acetate in 180 mL anhydrous ethanol and the solution was stirred for 4 h at room temperature. In turn, 0.1 g of $NaBH_4$ dissolved in 20 mL ethyl alcohol was added to the metal solution and vigorously stirred for 4 h. After finishing the stirring, the emulsion was filtered and washed several times and the remaining powders were dried at 60 °C oven for 12 h. Dried powders were then heat treated by tube furnace. The heat treatment was carried out at 300 °C for 3 h at N_2 atmosphere.

2.2 Electrochemical half-cell measurements

Electrochemical measurements were carried out using a computer connected potentiostat (CHI 720D, CH Instrument, USA). For the three-electrode cell measurements like CV and RDE, Pt wire was used as a counter electrode and Ag/AgCl (soaked in 3M KCl) was used for a reference electrode. To make working electrode, catalytic powder was mixed with isopropanol and 5 wt. % Nafion solution under sonication for 10 min. After mixing, the catalytic ink was dropped on glass carbon disk electrode with loading amount of 8 µL. After loading, the working electrode was dried for 1 h at room temperature. 1.0 M H_2SO_4 was used as an electrolyte to promote oxygen reduction reaction and high purity N_2 and O_2 gases were bubbled to the electrolyte to create a specific atmosphere like lacking in O_2 (with N_2 bubbling) or enriched O_2 (with O_2 bubbling). All the tests were performed at room temperature.

To evaluate the reduction reaction capability of Pt/C and PtM/C catalysts, CV and LSV curves using RDE were measured. In CV tests, while 1.0 M H_2SO_4 was used as electrolyte, potential scan range was from -0.23 to 1.0 V vs. Ag/AgCl and potential scan rate was 50 mV s^{-1}. These tests were performed in the presence of O_2 and N_2 gases, respectively. For obtaining the LSV curves, 1.0 M H_2SO_4 solution was used as an electrolyte in the presence of O_2 gas and rotating speed of RDE was varied from 200 to 1000 rpm and potential scan rate was 10 mV s^{-1}.

For estimating catalytic stability of the catalyst candidates, the accelerated durability test (ADT) was performed using CV [8]. While running ADT, the corresponding samples underwent multiply reiterated CVs. For this test, 1.0 M H_2SO_4 was used as an electrolyte, while N_2 gas was continuously supplied to remove O_2 from the electrolyte. Potential scan range of the CVs was from -0.23 to 1.0 V vs. Ag/AgCl and scan rate was 50 mV s^{-1}.

2.3 Electrochemical single-cell measurements

For PEMFC single cell tests, membrane electrode assemblies (MEAs) with active area of 5.0 cm^2 were prepared. Pt/C was introduced as anodic catalyst, while Pt/C and PtM/Cs were assigned as cathodic catalysts, respectively. The catalyst powders of Pt/C and PtM/Cs were ultrasonically mixed with 5 % Nafion solution (Solution Technology, Inc., 1100EW) and deionized with water and isopropyl alcohol for the preparation of catalyst ink. For making MEA, CCM (catalyst coated membrane) method was used. In the method, the catalysts inks were directly air-sprayed onto both sides of Nafion 212 (Dupont) membrane. The loading of metal catalysts were 0.2 mg cm^{-2} in both electrodes, respectively. The MEAs were then assembled with gas diffusion layers (GDL, E-Tek division, plane weave, 0.35 mm cloth thickness and 30% polytetrafluoroethylene (PTFE)) and gasket (TF 350, CNL, Inc.). The completed MEAs were then placed between two graphite plates, which have engraved serpentine flow channels.

After the single cell was assembled, it was installed at a fuel cell test station (Fuel cell control system, CNL, Inc.) for PEMFC test. While the PEMFC single cell test, cell temperature was maintained as 65 °C under 1atm, while 100 % humidified H_2 gas and air were provided to anode and cathode with a stoichiometric ratio of 1.5:2, respectively.

2.4 Characterization of Catalysts

XRD measurements were implemented using a Rigaku Mini Flex II using Cu K$_\alpha$ radiation (λ = 1.5418 Å). All the data were recorded in the range of 2θ = 10-90 ^{o}C at 30 kV and 15 mA. Elemental composition of catalysts was determined by EDX measurement using Hitachi S-4200 at 20 kV, 3 K magnification and spot size of 2. Particle size and dispersion of catalysts were confirmed by TEM (Philips, CM30, at 200 kV).

3. RESULTS AND DISCUSSION

*3.1 Evaluations for crystal structure and elementary composition of the PtM catalysts*

To investigate crystal structure and elementary composition of PtM/C and Pt/C catalysts, XRD, TEM and EDX measurements were carried out. Fig. 1 indicates TEM images and EDX measurements of PtM/C catalysts. According to them, nanoparticles of PtNi, PtCo and PtCu were well dispersed. Atomic and weight percent of PtM catalysts were estimated from EDX spectra and they are summarized in Table 1. In terms of the atomic percent, the three PtM (M= Ni, Co and Cu) alloys consisted of almost one-to-one ratio of Pt and M, indicating that all the PtM alloys were existed as a stoichiometric ratio of Pt_1M_1. When it comes to the weight percentage, weight fraction of Pt in the three PtM alloys was 14.8 ~ 20.1 % (see Table 1). Compared to commercial Pt/C (40 wt.%), portion of the Pt in the PtM alloys is far less.

**Table 1.** Atomic percent and weight percent of PtM (M = Ni, Co and Cu) catalysts.

	Pt At. %	M At. %	Pt Wt. %	M Wt. %
PtNi/C	1.62	1.21	20.06	4.53
PtCo/C	1.12	0.81	15.06	2.05
PtCu/C	1.15	1.36	14.83	5.71

It is noticeable that in case of PtY alloy, Y component was not detected by EDX measurement, meaning that Y was not properly alloyed with Pt when reduction method by NaBH$_4$ was used. It was previously reported that PtY was mainly alloyed by high pressure rf magnetron sputtering, not by chemical treatment [17].

Fig. 2 shows powder XRD patterns of PtM/C (M= Ni, Co, Cu and Y) catalysts. According to the XRD pattern, four main peaks of PtMs, which were shown in 40°, 47°, 68°, and 82° , corresponded to (111), (200), (220) and (311) planes of face centered cubic (fcc) structure of Pt. The peaks all shifted higher angle than those of Pt/C.
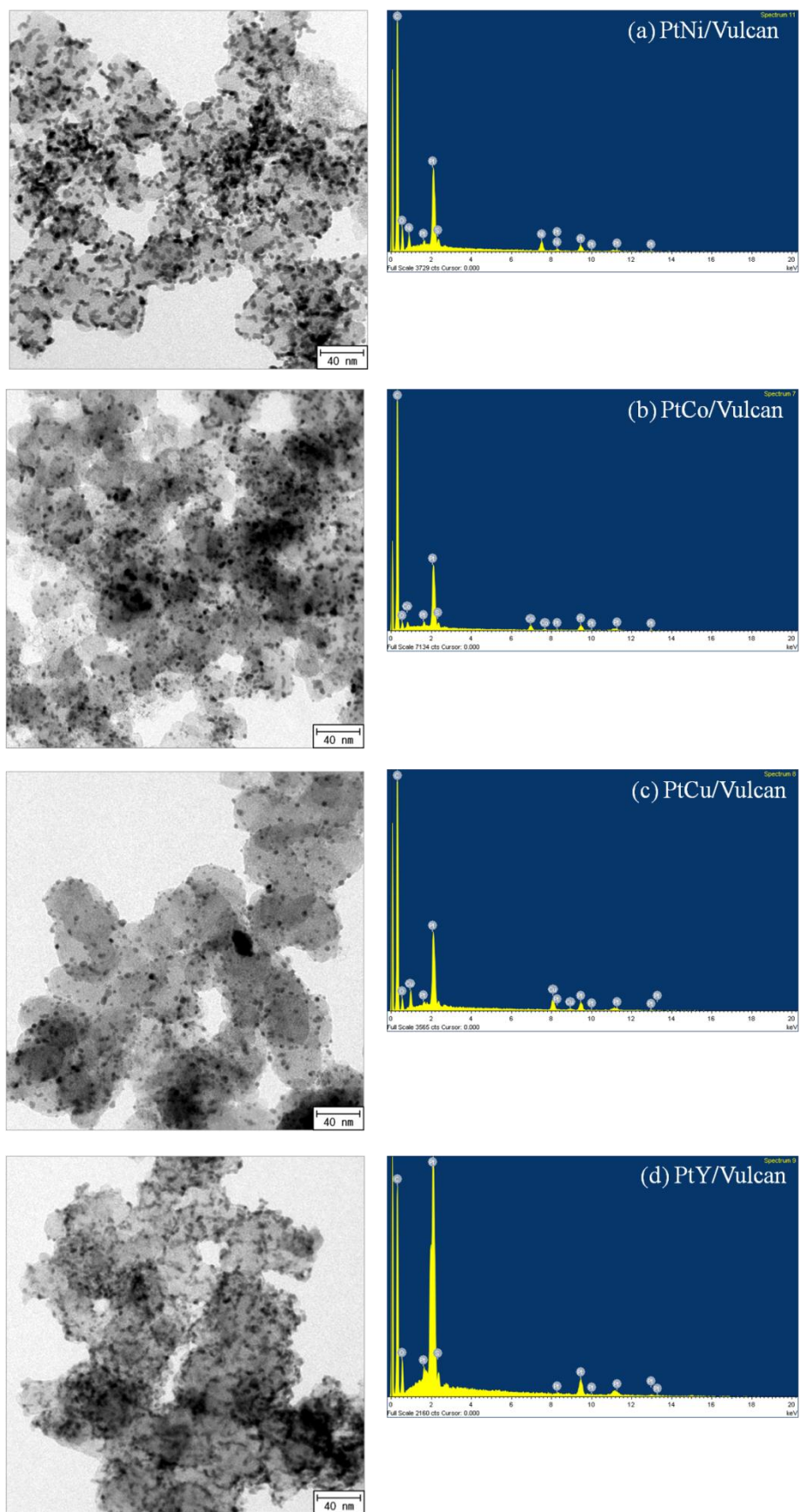
Figure 1. TEM images (left) and EDX spectrum (right) of (a) PtNi/C, (b) PtCo/C, (c) PtCu/C and (d) PtY/C catalysts.
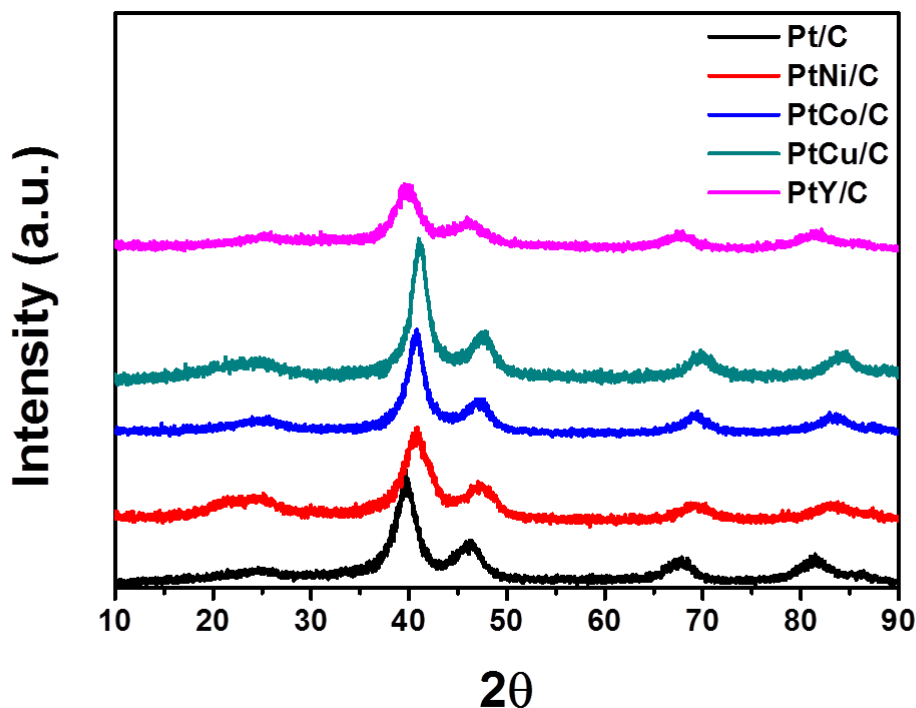
Figure 2. XRD patterns for Pt/C and PtM (M = Ni, Co, Cu and Y) catalysts.

It means that contraction between lattices of the Pt-M alloy occurs during the formation of PtM alloy, indicating that the interatomic distance between Pt atoms is reduced due to the replacement of Pt by small-sized transition metal M. The average particle size of the PtM/Cs was also calculated by using Scherrer's equation with the XRD peak assigned to Pt (220) [19,20]. In PtNi/C, PtCo/C and PtCu/C, particle size was 4.3, 5.8 and 6.3 nm, respectively. The particle size of PtMs was also compatible with that in Pt/C (5.4 nm).

Alloying degrees of the PtM/Cs were also calculated by XRD using Vegard's law [21,22]. According to the law, in the XRD pattern of PtM/Cs, the Pt (220) peak was selected for the determination of lattice parameter that was one of requisite factors to calculate alloying degree of the PtM/Cs because the peak was far from the background signal of carbon support [19,22]. The lattice parameter ($a_{(220)}$) of PtM/Cs was initially obtained by a combination of the Pt (220) peak position (θ_{max}) and the wavelength of Cu K_α radiation ($\lambda_{\kappa\alpha}$)

$$a_{(220)} = 2^{0.5}\lambda_{\kappa\alpha}/\sin\theta_{max} \qquad\qquad (1)$$

In turn, the alloying degrees of PtM/Cs were expressed as a function of (i) Pt atomic fraction (X_{Pt}) in the PtM/Cs and (ii) nominal Pt/M atomic ratio ($(Pt/M)_{nom}$) that were attained by the lattice parameter and the EDX measurement, respectively, with the following equations.

$$a_{(220)} = 3.8013 + 0.124x_{pt} \qquad\qquad (2)$$

$$\text{Alloying degree} = x_{pt}/(1-x_{pt})(Pt/M)_{nom} \qquad\qquad (3)$$

Table 2 summarizes Pt(200) peak position, atomic fraction of Pt in PtM/Cs and alloying degree of the PtM/Cs. As a result of that, alloying degrees of PtNi/C, PtCo/C and PtCu/C calculated were 44, 50 and 9 %, respectively.

Table 2. Pt(200) peak position of PtM/Cs, atomic fraction of Pt in PtM/Cs and alloying degree of PtM/Cs.

	2Θ (degree)	a(220)	x_{pt}	Alloying degree
PtNi/C	69.043	3.847	0.37	44%
PtCo/C	68.928	3.853	0.41	50%
PtCu/C	69.814	3.810	0.07	9%

3.2 ORR activity and catalytic stability of the PtM/C catalysts
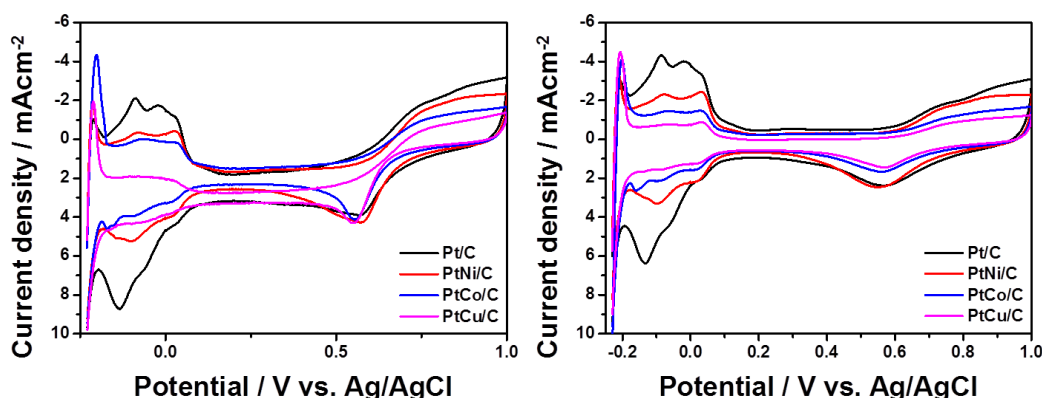
Figure 3. CV curves of Pt/C and PtM (M = Ni, Co and Cu) catalysts that were in the presence of (a) N_2 and (b) O_2 gases, respectively. For the tests, 1.0 M H_2SO_4 solution was used as an electrolyte with scan rate of 10 mV s^{-1}.

To investigate the reduction reaction capability of the PtM/C catalysts and compare them with that of Pt/C, CV and RDE curves of the PtM/Cs and Pt/C were measured. Of them, CV results are shown in Fig. 3a-b. In the CV curves, typical ORR peak of all the PtM/C catalysts clearly appeared at potential range of 0.5~0.6 V vs. Ag/AgCl in the presence of O_2 gas (see Fig. 3a). In terms of both limiting current density and ORR peak potential, all the PtM/C catalysts showed very similar values to Pt/C catalyst (see Table 3 for the exact values). CVs of PtM/Cs and Pt/C measured in the presence of N_2 enabled calculation of EAS. Properly defined hydrogen adsorption peak was appeared at the potential range of -0.23 ~ 0.1 V vs. Ag/AgCl, while oxidation and reduction peaks existed at the potential range of 0.4 ~ 1.0 V vs. Ag/AgCl. The EASs of all the catalysts are decided by the following equation.

$$EAS = Q/mq \qquad (4)$$

Where, Q is the charge of hydrogen adsorption and q is the charge required for monolayer adsorption of hydrogen on the Pt surface (Pt oxidation), while m is the loading amount of metal catalyst. With assumption that a monolayer of hydrogen is adsorbed on the Pt surface, q is considered

210 µC cm^{-2} [19]. The EASs calculated for Pt, PtNi, PtCo and PtCu was 43.5, 37.6, 37.5 and 24.0 m^2 g^{-1}, respectively, indicating that it was ranked as the order of Pt > PtNi > PtCo > PtCu.

Table 3. ORR peak potential, half wave potential, maximum current density, maximum power density, maximum current density per gram Pt and maximum power density per gram Pt that were measured by CV, LSV and PEMFC single cell when PtM/Cs (M = Ni, Co and Cu) were used for ORR catalysts.

	CV		RDE			PEMFC	
	Peak potential	Maximum current density	half wave potential	Maximum current density	Maximum current density per mg$_{Pt}$	Maximum power density	Maximum power density per mg$_{Pt}$
	[V]	[mAcm^{-2}]	[V]	[mAcm^{-2}]	[mAmg$_{pt}^{-1}$ cm^{-2}]	[Wcm^{-2}]	[Wmg$_{pt}^{-1}$ cm^{-2}]
Pt/C	0.570	6.320	0.588	2.461	61.535	0.517	2.587
PtNi /C	0.571	4.277	0.604	2.432	121.272	0.587	5.874
PtCo /C	0.555	4.121	0.599	1.751	116.275	0.419	5.588
PtCu /C	0.551	4.307	0.580	1.996	134.644	0.448	5.980

Based on the CVs measured in the presence of N$_2$, onset points in the Pt oxidation (Pt + H$_2$O → Pt-OH + H$^+$ + e$^-$) of all the catalysts were also investigated. It was usually admitted that Pt-OH was produced by oxidation of water on Pt surface at higher potential than 0.7 V vs. Ag/AgCl [9]. As shown in Fig. 3b, the extent of Pt-OH production was ranked as the order of Pt > PtNi > PtCo > PtCu. It indicated that Pt-OH in PtM catalysts was less produced than that in Pt/C catalyst. According to Rao *et al.*, less production of Pt-OH in the PtM catalysts was due to the combination between low electron occupancy in d orbital of M and high electron occupancy in d orbital of Pt [9]. The coupling caused reduction in density of state (DOS) at Fermi level of Pt and down shift in center energy of Pt d-band. In this situation, M atom in PtM acted as an electron donor to Pt atom. The Pt atom that accepted electron from M atom took on negative charge, while M atom was positively charged. Such a charge distribution induced strong interaction between M atom (positively charged) and O of the adsorbed OH group (negatively charged). The DOS reduced at Fermi level of Pt by electron transfer from M atom weakened covalent bonds between Pt and OH group, enhancing oxygen reduction reaction. Eventually, the reduction of DOS in PtM leads to the oxygen adsorption at low overpotential, followed by improved ORR kinetics.

To confirm whether the CV results on the effect of PtM/Cs on ORR were valid, LSV curves of all the catalysts using RDE were measured. Fig. 4 presents the LSV curves. Data over limiting current density and half wave potential of the catalysts were summarized in Table 3. In both limiting current density and half wave potential, the value of Pt/C and PtNi/C was higher than that of other PtM/C catalysts. Taken together, electrochemical ORR performance collected from LSV and CV curves such as EAS, potential for onset of Pt-OH formation, limiting current density and half wave potential were

well agreed each other. Indeed, although the amount of Pt in PtM/C was far less than that in Pt/C, ORR performances of PtM/Cs were still worse than those of Pt/C.
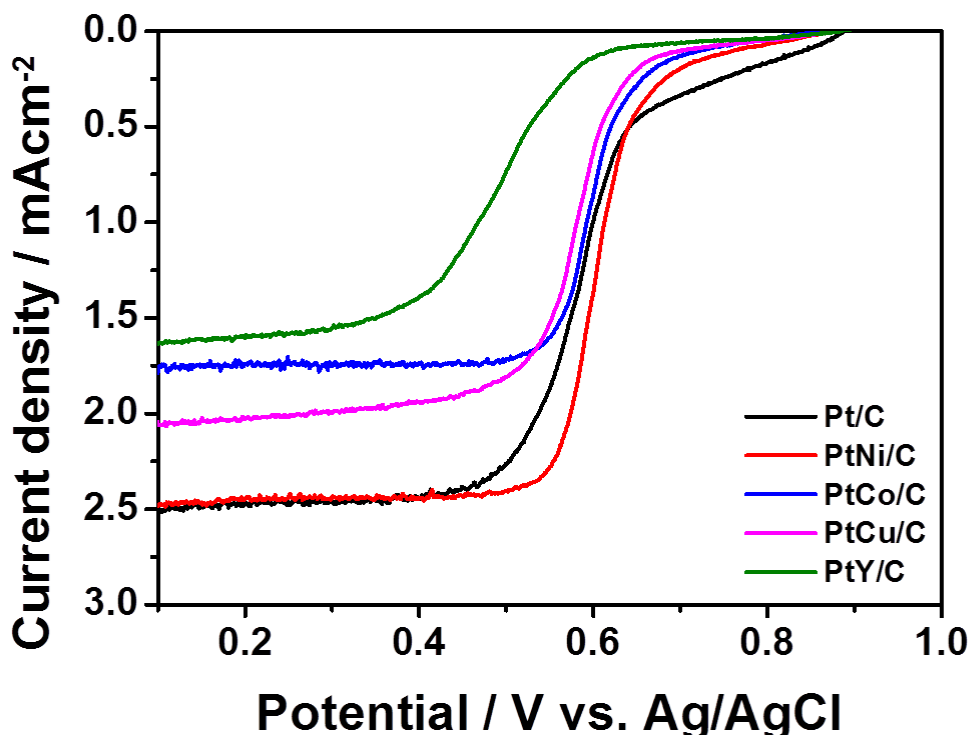
Figure 4. LSV curves using RDE of the four different catalysts (Pt/C and PtM (M = Ni, Co and Cu)). 1.0 M H_2SO_4 solution was used as an electrolyte in O_2-saturated state with scan rate of 10 mV s^{-1} and rotation speed of 1000 rpm.

To further evaluate the effect of PtM/Cs on ORR, transferred electron number n per oxygen molecule and kinetic current density were measured. The n-value and kinetic current density were obtained with adoption of the Koutechy-Levich (K-L) equation that was given below [24,25].

$$1/j = 1/j_k + 1/B\omega^{0.5} \tag{5}$$

Here, j and ω are the applied current density and the electrode rotating rate, respectively. The ω is an input parameter. j_k (kinetic current density) and B are determined as an intercept of y direction and a slope in the relationship between $1/j$ and $1/\omega^{0.5}$. Once B is determined, n is calculated from the following Levich equation [24].

$$n = B/(0.2F(D_{O2})^{2/3}v^{-1/6} C_{O2}) \tag{6}$$

Where F is Faraday's constant (96485 $Cmol^{-1}$), D_{O2} is the diffusion coefficient of O_2 in 0.1M H_2SO_4 (1.4×10^{-4} cm^2sec^{-1}), v is the kinetic viscosity (0.01 cm^2sec^{-1}) and C_{O2} is the bulk concentration of O_2 (1.16×10^{-6} mol cm^{-3}). The constant 0.2 is employed when the rotation speed is expressed in rpm [26].

To get n-value, LSV curves using RDE whose rotation speed was increased from 200 to 1000 rpm were measured for the PtM/C and Pt/C catalysts and their correlation between $1/j$ and $1/\omega^{0.5}$ were displayed in Fig. 5a-d. In all the catalysts, $1/j$ had a linear relationship with $1/\omega^{0.5}$ at the potentials of

0.2 ~ 0.4 V vs. Ag/AgCl which were partly overlapped with potential range for ORR. In turn, j_k, B and n were attained by uses of Eqs. 5 and 6. In the result, average n-value of Pt/C reached almost 4.0, while the values of PtNi/C, PtCo/C and PtCu/C were 3.4, 2.8 and 3.4, respectively. When it comes to j_k, the average values of Pt/C, PtNi/C, PtCo/C and PtCu/C were 0.994, 1.367, 0.855 and 0.628 mAcm^{-2}. Based on that, it was concluded that Pt/C satisfied the four-electron ORR pathway for producing H_2O without formation of intermediate H_2O_2 in that n-value was near to four, whereas PtM/C catalysts fell short of their goal - the four-electron ORR pathway for producing H_2O. Also, j_k s for Pt/C and PtNi/C were better than those of other PtM/Cs.
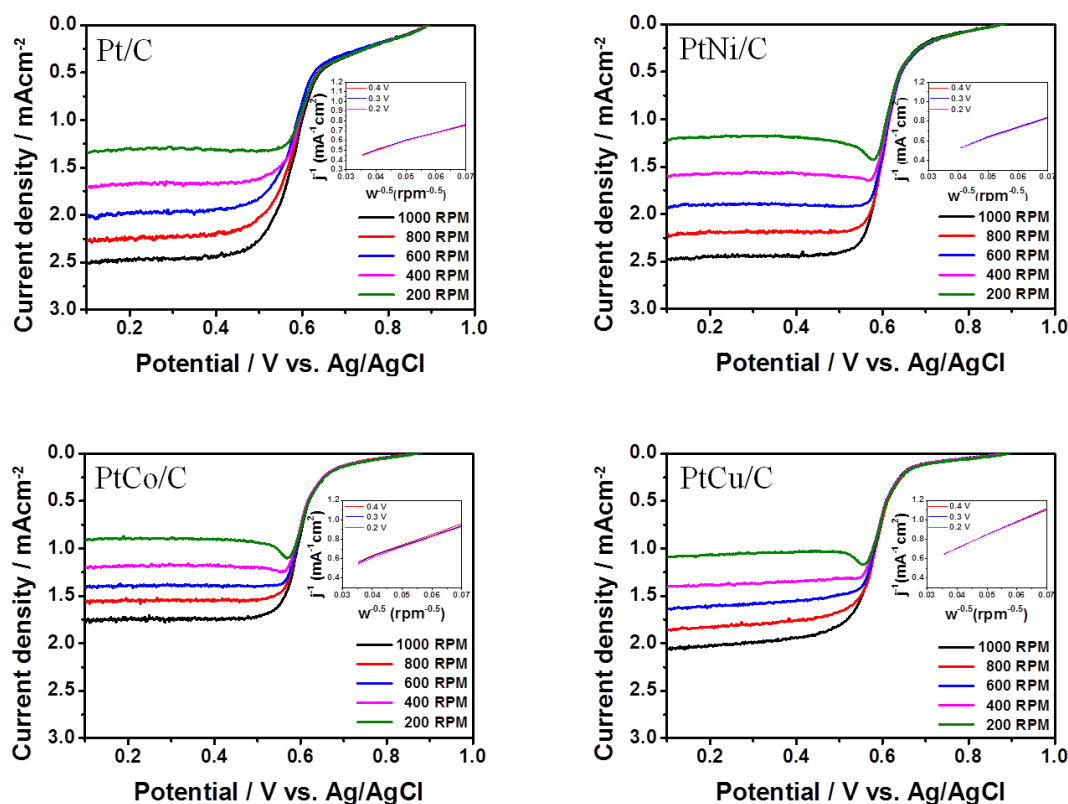
Figure 5. LSV curves obtained by changes in the rotation speed of RDE in the four different catalysts (Pt/C and PtM (M = Ni, Co and Cu)). Insets indicated K-L plots showing the linear relationship between 1/j and $1/\omega^{0.5}$ of the catalysts. Rotation speed of the RDE was varied from 200 to 1000 rpm. For the tests, 1.0 M H_2SO_4 solution was used as an electrolyte in O_2-saturated state with scan rate of 10 mV s^{-1}.

It is instrumental to explore catalytic stability as well as ORR activity of PtM/C catalysts acting as the substitute of Pt/C catalyst. For the purpose, catalytic stability of PtM/C catalysts was measured by ADT and the data was compared with that of Pt/C catalyst. In the ADT test, 400~500 cycles of CV were run repeatedly and EASs of the PtM/Cs and Pt/C were measured once per every 100 turns of CV. Fig. 6a-d shows the CV curves. According to the CVs, loss in EAS of the catalysts consecutively occurred with run of CV in all catalysts and after 400 cycle, relative EASs (present EAS / initial EAS) of PtM/Cs were higher than that of Pt/C as an order of PtCu/C, PtCo/C, PtNi/C and Pt/C. Fig. 6e

indicates a relationship between loss rate in EAS and number of CV cycle in all catalysts. In the figure, loss rates in EAS of PtM/Cs were far lower than that of Pt/C within the given cycle range. This means that PtM/Cs have better long term stability (lifetime) than Pt/C.
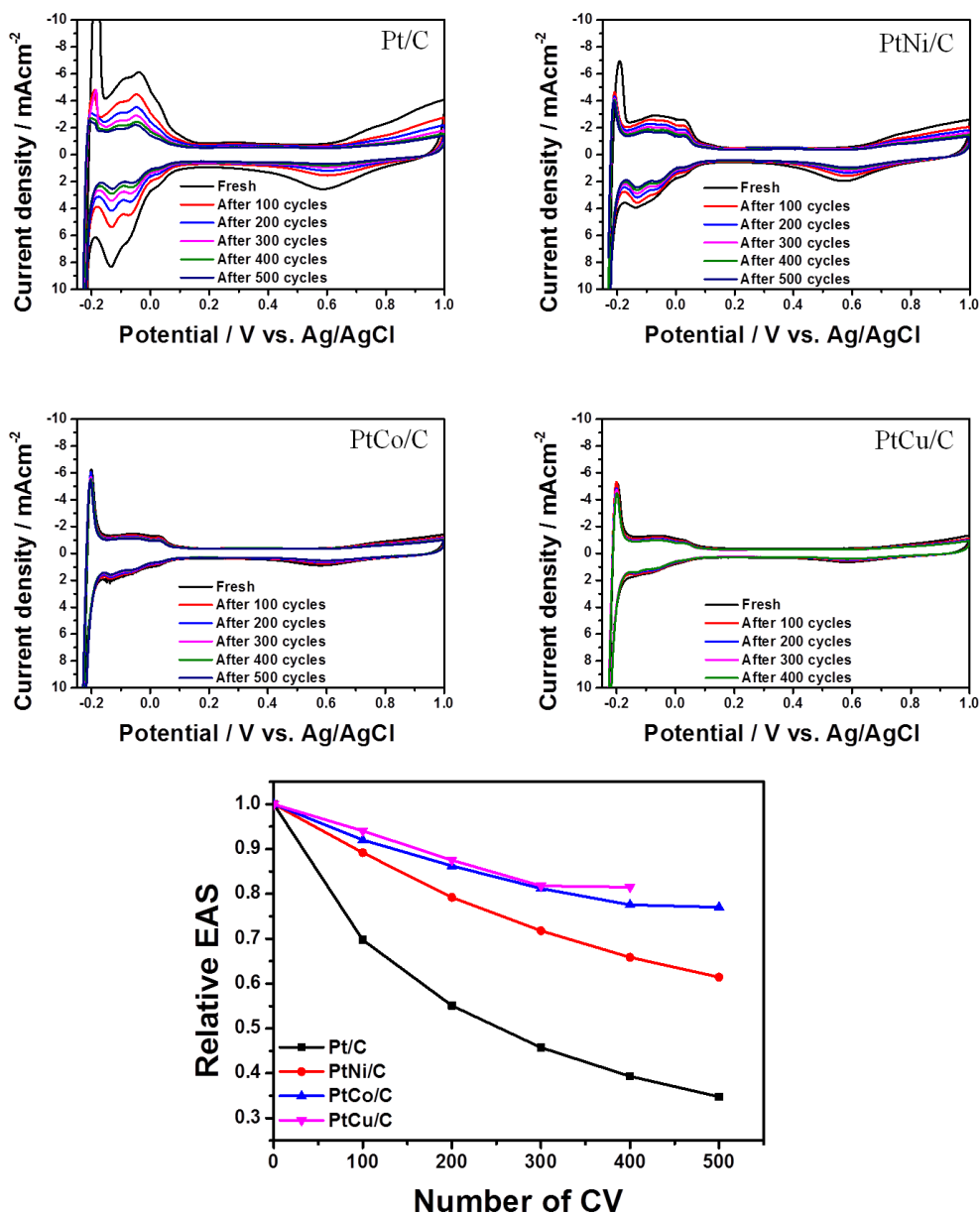

Figure 6. CV curves of (a) PtNi/C, (b) PtCo/C, (c) PtCu/C and (d) Pt/C. CVs of the most catalysts were cycled for 500 turn except PtCu/C (The PtCu/C catalyst was cycled for 400 turn). For the tests, 1.0M H_2SO_4 solution was used as an electrolyte in N_2-saturated state. Potential scan range of the CVs was from -0.25 to 1.0 V vs. Ag/AgCl and scan rate was 50 mV s^{-1}. The effect of relative EAS on the number of CV in all the catalysts was estimated in Fig. 6e.

More degradation of the long term stability in Pt/C than PtM/Cs could be explained by the following two ways; first, influence of dissolution rate of the corresponding metal particles on carbon corrosion and second, agglomeration of Pt particles by Oswald ripening. According to Marcus [27], the

difference in dissolution rate of metals depended on (i) adsorption energy for oxygen-metal bond and (ii) metal-metal bond energy. As the adsorption energy for oxygen-metal bond was getting decrease and metal-metal energy is getting increase, the metal is prone to dissolve. Since Pt has lower adsorption energy for oxygen-metal bond and higher metal-metal bond energy than M metals (M= Ni, Co and Cu), dissolution rate of Pt was higher than that of other M metals. Also, with Oswald ripening effect of Pt, the Pt atoms were dissolved and moved into other Pt atoms to produce large Pt particles, remaining carbon supporter vulnerable. When metal particles dissolved, corrosion reaction occurred in carbon supporter of the dissolved catalysts as given in Eq. 7 [8].

$$C + 2H_2O \rightarrow CO_2 + 4H^+ + 4e^- \tag{7}$$

It was theoretically suggested that dissolution rate of Pt/C catalyst was higher than that of PtM/Cs because corrosion in carbon supporter of Pt/C was more likely to happen than that of PtM/Cs, demonstrating that catalytic stability of PtM/Cs was certainly better than that of Pt/C.
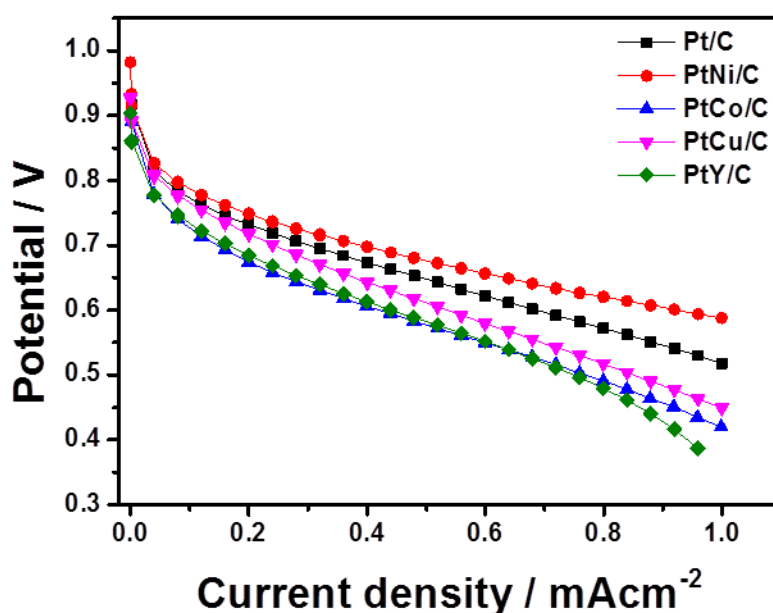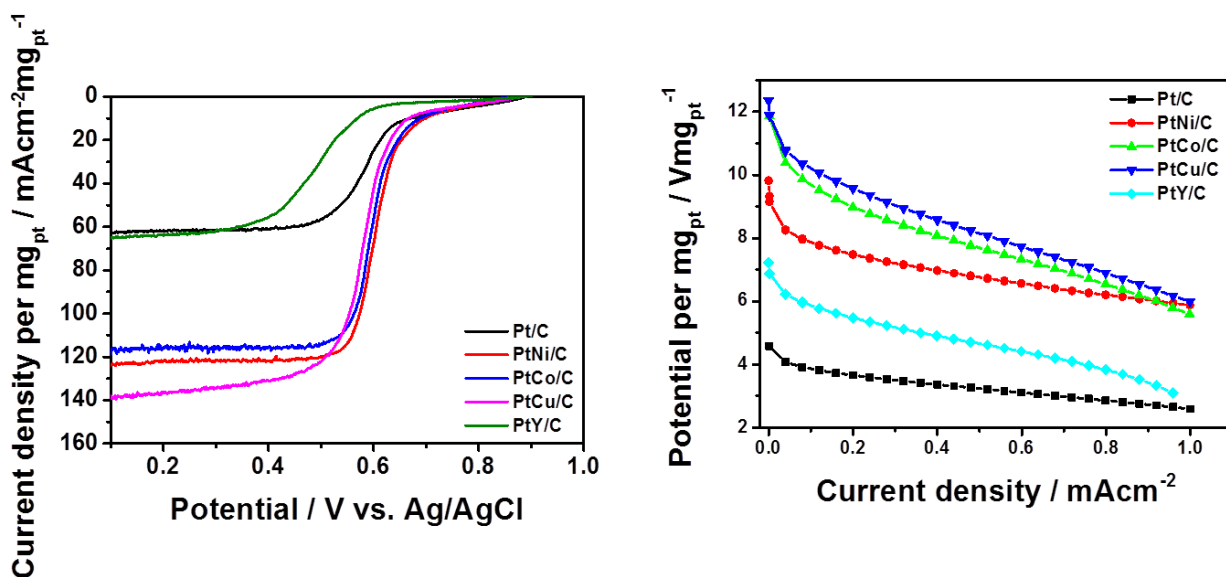

Figure 7. Polarization curves of PEMFC single cells using the four different materials (Pt/C and PtM (M = Ni, Co and Cu)) as cathodic catalysts. For the tests, CCM method was used for making MEA with the loading amount of 0.2 mg cm^{-2} in both electrodes. While the PEMFC single cell tests, the cell temperature was maintained as 65°C under 1atm and 100% humidified H$_2$ gas and air were provided to anode and cathode with a stoichiometric ratio of 1.5:2.

Effect of Pt/C and PtM/C catalysts on electrical performance of PEMFC single cell was investigated. For obtaining polarization curve from the single cell tests, the same amount of metal catalysts for both anode (0.2 g$_{Pt/C}$ cm^{-2}) and cathode (0.2 g$_{PtM/C}$ cm^{-2}) were loaded. The polarization curves are presented in Fig. 7. Amid the catalysts tested, electrical performance of single cell using PtNi/C was greater than that using Pt/C, although the performances of PtCo/C and PtCu/C did not yet reach the same level to that of Pt/C. open circuit potentials (OCPs) of Pt/C, PtNi/C, PtCo/C and PtCu/C were 0.92, 0.98, 0.90 and 0.93V, while maximum power densities (MPDs) of them were 0.518,

0.59, 0.42 and 0.45 Wcm^{-2}. These single cell results were well agreed with CV and RDE results of Figs 3 and 4, explaining that PtNi/C had better ORR activity than Pt/C.

3.3 ORR mass activity per gram Pt for the PtM/C catalysts

By the experiments for measuring ORR activities of PtM/C catalysts, it was found that all the PtM/Cs showed better catalytic stability than Pt/C, while ORR activity and PEMFC performance of PtNi/C were excellent. Here, it deserves to notify that all the PtM/Cs consist of smaller amount of Pt than Pt/C (see Fig. 1). Due to the reason, it is needed to elucidate whether performance per gram Pt included in PtM catalysts indicates the similar trend to performance of the entire PtM catalysts. Data over the performance per gram Pt are related to the extent of actual utilization of Pt affecting cost paid for synthesizing the corresponding catalyst.

Figure 8. (a) LSV curves using RDE of the four different catalysts (Pt/C and PtM (M = Ni, Co and Cu)) and (b) Polarization curves of PEMFC single cells using the four different materials (Pt/C and PtM (M = Ni, Co and Cu)) as cathodic catalysts. Unlike Figs. 4 and 7, the corresponding LSV and polarization curves were evaluated by "per gram Pt".

To explore ORR mass activity and performance per gram Pt in all the catalysts, LSV curves of Fig. 4 and polarization curves of Fig. 7 were redefined as "per gram Pt" and the results are presented in Fig. 8. In Fig. 8a, the LSV curves of per gram Pt of all the catalysts were totally different from those of Fig. 4. When it comes to limiting current density, the values of PtM/C (M= Ni, Co and Cu) were higher than Pt/C by a factor of two. At the same manner, the polarization curves of per gram Pt of all the catalysts (Fig. 8b) showed the same tendency to the LSV curves of Fig. 8a, indicating MPDs of per gram Pt of PtM/C were greater than that of Pt/C. MPDs per gram Pt of Pt/C, PtNi/C, PtCo/C and PtCu/C were 2.59, 5.87, 5.59 and 5.98 Wg_{Pt}^{-1}cm^{-2}. Both LSV and polarization curve results supported the fact that Pt particles in PtM/C catalysts were more utilized than those in Pt/C.

4. CONCLUSIONS

We proposed carbon supported PtM (M = Ni, Co, Cu and Y) alloy as cathodic catalysts for PEMFCs and their ORR activity, catalytic stability and electrical performance were probed and compared with those of 40 wt. % Pt/C. The crystal structure, elementary composition and alloying degree of them were measured by XRD, EDX and TEM. According to TEM and XRD measurements, particle size of PtM/Cs was similar to that of Pt/C and alloying degree of PtMs was completed in a moderate level. In addition, EDX measurement indicated that PtMs were existed as a stoichiometric ratio of Pt_1M_1.

To inspect ORR activity and catalytic stability of catalysts, CV and RDE were used. In tests for measuring ORR activity, only PtNi/C showed better limiting current density, kinetic current density, half wave potential and reduction peak potential than Pt/C, while catalytic stabilities of all the PtM/Cs were better than that of Pt/C. It might be because of higher adsorption energy for oxygen-M bond and lower M-M bond energy.

Even in PEMFC single cell test, MPD of PEMFC single cell employing PtNi/C was better than that of PEMFC single cell employing Pt/C although other PtM/Cs showed worse MPDs. However, when the measurements are estimated as per gram Pt, the trend was totally changed, meaning that all the PtM/C catalysts showed better MPDs than Pt/C, proving that Pt particles in PtM/C were more effectively utilized than those in Pt/C.

References

1. T. Toda, H. Igarashi, H. Uchida and M. Watanabe, *J. Electrochem Soc.*, 146 (1999) 3750.
2. T.Y. Jeon, S.J. Yoo, Y.H. Cho, K.S. Lee, S.H. Kang and Y.E. Sung, *J. Phys. Chem. C*, 113 (2009) 19732.
3. Z. Yang, H. Nie, X. Chen, X. Chen and S. Huang, *J. Power Sources*, 183 (2008) 34.
4. C. Wang, N.M. Markovic and V.R. Stamenkovic, *ACS Catal.*, 2 (2012) 891.
5. H.-S. Oh, J.-G. Oh, W.H. Lee and H. Kim, *J. Mater. Chem.*, 22 (2012) 15215.
6. T.Y. Jeon, N. Pinna, S.J. Yoo, S.-H. Yu, S.-K. Kim, S. Lim, D. Peck, D.-H. Jung and Y.E. Sung, *J. Electroanal. Chem.*, 662 (2011) 70.
7. H.-S. Oh, J.-G. Oh, B. Roh, I. Hwang and H. Kim, *Electrochem. Commun.*, 13 (2011) 879.
8. D.He, S. Mu and M. Pan, *Carbon*, 49 (2011) 82.
9. C.V. Rao and B. Viswanathan, *J. Phys. Chem. C*, 113 (2009) 18907.
10. S. Mukerjee and S. Srinivasan, *J. Electroanal. Chem.*, 357 (1993) 201.
11. L. Xiong, A.M. Kannan and A Manthiram, *Electrochem. Commun.*, 4 (2002) 898.
12. H.T. Duong, M.A. Rigsby, W.P. Zhou and A. Wieckowski, *J. Phys. Chem. C*, 111 (2007) 13460.
13. H. Yano, M. Kataoka, H. Yamashita, H. Uchida and M. Watanabe, *Langmuir*, 23 (2007) 6438.
14. S. Mukerjee, S. Srinivasan, M.P. Soriaga and J. McBreen, *J. Electrochem. Soc.*, 142 (1995) 1409.

15. E. Antolini, J.R.C. Salgado, M.J. Giz and E.R. Gonzalez, *Int. J. Hydrogen Energy*, 142 (2005) 1213.
16. H.S. Oh, K. Kim and H. Kim, *Int. J. Hydrogen Energy*, 36 (2011) 11564.
17. S.J. Yoo, S.-K. Kim, T.-Y. Jeon, S.J. Hwang, J.-G. Lee, S.-C. Lee, K.-S. Lee, Y.-H. Cho, Y.-E. Sung and T.-H. Lim, *Chem. Commun.*, 47 (2011) 11414.
18. C. Wang, M. Chi, D. Li, D.V.D. Vilet, G. Wang, Q. Lin, J.F. Mitchell, K.L. More, N.M. Markovic and V.R. Stamenkovic. *ACS Catal.*, 1 (2011) 1355.
19. C.V. Rao, A.L.M. Reddy, Y. Ishikawa and P.M. Ajayan, *Carbon*, 49 (2011) 931.
20. S. Maass, F. Finsterwalter, G. Frank, R. Hartmann and C. Merten, *J. Power Sources*, 176 (2008) 444.
21. D. Wang, L. Zhuang and J. Lu, *J. Phys. Chem. C*, 111 (2007) 16416.
22. E. Antolini and F. Cardellini, *J. Alloys Compd.*, 315 (2001) 118.
23. S. Ozenler, N. Sahin, B. Akaydin, L. Ovecoglu, A. Genc, J-M. Léger, T.W. Napporn, and F. Kadirgan, *ECS Trans.*, 41 (2011) 1031.
24. S. Wang , D. Yu and L. Dai, *J. Am. Chem. Soc.*, 133 (2011) 5182.
25. S. Wang, L. Zhang, Z. Xia, A. Roy, D.W. Chang, J.B. Baek and L. Dai, *Angew. Chem. Int. Ed.*, 51 (2012) 4209.
26. S. Wang, D. Yu, L. Dai, D.W. Chang and J.B. Baek, *ACS Nano*, 5 (2011) 6202.
27. P. Marcus, *Corros. Sci.*, 36 (1994) 2155.